Articles

$[Pt_2(dppf)_2(\mu\text{-}S)_2]$ as a Heterometallic Ligand. Simple Assembly of an Electroactive Interpolymetallic Complex $[Pt_2Tl(dppf)_2(\mu_3\text{-}S)_2]X$ (X = NO_3, PF_6) (dppf = 1,1′-bis(diphenylphosphino)ferrocene)

Meisheng Zhou,* Yan Xu, Ai-Min Tan, Pak-Hing Leung, K. F. Mok, Lip-Lin Koh, and T. S. Andy Hor*

Department of Chemistry, Faculty of Science, National University of Singapore, Singapore 0511

Received June 2, 1995[⊗]

Facile complexation of a heterometallic ligand $Pt_2(dppf)_2(\mu\text{-}S)_2$ (dppf = 1,1′-bis(diphenylphosphino)ferrocene) with $TlNO_3$ gives $[Pt_2Tl(dppf)_2(\mu_3\text{-}S)_2]NO_3$, which metathesizes with NH_4PF_6 to give its PF_6^- salt. This Lewis acid−base addition forms the basis of an assembly of electroactive interpolymetallic aggregates which are constituted of an unsaturated fragment of a p-block metal and two redox-active Pt^{II} cores, linked by two flexible sulfide bridges. Intermetallics of other metals, *viz.* $Pt_2(dppf)_2(\mu_3\text{-}S)_2InCl_3$ and $[Pt_2(dppf)_2(\mu_3\text{-}S)_2Pb(NO_3)]NO_3$, are similarly assembled. The X-ray molecular structure of $[Pt_2Tl(dppf)_2(\mu_3\text{-}S)_2]PF_6$ reveals a side-on attachment of the ligand thereby exposing an "empty space" on the Tl^I atom. $[Pt_2Tl\{(C_5H_4PPh_2)_2Fe\}_2(S)_2]PF_6$: *a* 17.795(4), *b* 10.553(2), *c* 17.936(4) Å; monoclinic; *P2/n*; Z 2. No direct Pt−Tl bonding is envisaged but the close contacts between the two atoms (3.389(1) Å) enable $^{195}Pt-^{203/205}Tl$ coupling to be observed in the ^{195}Pt NMR spectrum. The electrochemical behavior of this complex is examined by cyclic voltammetry in 1,2-dichloroethane. The complex undergoes an apparently irreversible two-electron-transfer process of the Tl^+ center and a quasi-reversible two-electron-transfer process involving two noninteracting ferrocenyl moieties.

Introduction

One major advantage for heteropolymetallics is the presence of several sites within a complex which are chemically unique but electrochemically communicative and catalytically cooperative. Among the common synthetic strategies developed for these complexes, the use of metalloligand as a precursor in Lewis acid-base reactions is probably the most effective and straightforward. The earlier use of $Pt_2(PPh_3)_4(\mu\text{-}S)_2$ (**1**) in

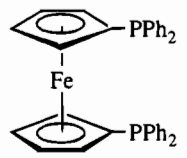

Dppf

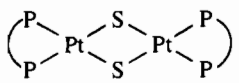

(P⌒P = 2 x PPh_3, **1**, dppf, **2**)

heterometallic syntheses[1] and our recent use in intermetallics[2] are illustrative of this approach. Structurally, these species comprise three major components:

a. Heterometal M. It is a key element in this molecular assembly. Its value lies in its unsaturation and redox activity, e.g., $Tl^I \rightleftharpoons Tl^{III}$, $Sn^{II} \rightleftharpoons Sn^{IV}$, *etc.*

b. Bridging sulfide. It is geometrically tailored to bring the two metals, M and Pt, to near-bonding separations. It is important that the sulfide links are adaptable to the change in M−Pt distances. The ability of sulfide to transmit electron charge efficiently also makes it an attractive ligand in complexes with good redox potential.

c. Pt core. The possibility for Pt^{II} to switch between a 16e and 18e configuration is an advantage. The presence of two Pt^{II} centers gives an added flexibility in the catalytic design.

These complex aggregates satisfied our earlier expectations in showing some unusual bonding and stereogeometric properties.[2] However, one major deficiency remains—neither their catalytic potential nor their redox activity has been demonstrated. In order to address this problem, we need to modify the Pt^{II} core since neither Pt^{II} nor its neighboring PPh_3 is renowned for its redox activity. An obvious solution, with minimum alterations to the synthetic pathway and product structures, is to introduce an electroactive fragment to the Pt^{II} core (Figure 1). This could be realized if $Pt_2(dppf)_2(\mu\text{-}S)_2$ [3] (**2**), is used instead of **1** as the synthon provided that it can show similar Lewis basicity. The chemistry of 1,1′-bis(diphenylphosphino)ferrocene (dppf) is rich and has recently been reviewed.[4] This ligand is known to confer its electroactivity to its complexes.[5]

In this paper, we describe the basicity of **2** toward a Lewis

[⊗] Abstract published in *Advance ACS Abstracts,* November 1, 1995.

(1) Briant, C. E.; Hor, T. S. A.; Howells, N. D.; Mingos, D. M. P. *J. Chem. Soc., Chem. Commun.* **1983**, 1118. Briant, C. E.; Hor, T. S. A.; Howells, N. D.; Mingos, D. M. P. *J. Organomet. Chem.* **1983**, *256*, C15. Briant, C. E.; Gilmour, D. I.; Luke, M. A.; Mingos, D. M. P. *J. Chem. Soc., Dalton Trans.* **1985**, 851. Gilmour, D. I.; Luke, M. A.; Mingos, D. M. P. *J. Chem. Soc., Dalton Trans.* **1987**, 335. Battistoni, C.; Mattogno, G.; Mingos, D. M. P. *Inorg. Chim. Acta* **1984**, *86*, L39. Aw, B. H.; Looh, K. K.; Chan, H. S. O.; Tan, K. L.; Hor, T. S. A. *J. Chem. Soc., Dalton Trans.* **1994**, 3177.

(2) Zhou, M.; Xu, Y.; Lam, C.-F.; Koh, L.-L.; Mok, K. F.; Leung, P.-H.; Hor, T. S. A. *Inorg. Chem.* **1993**, *32*, 4660. Zhou, M.; Xu, Y.; Lam, C.-F.; Leung, P.-H.; Koh, L.-L.; Mok, K. F.; Hor, T. S. A. *Inorg. Chem.* **1994**, *33*, 1572.

(3) Zhou, M.; Lam, C. F.; Mok, K. F.; Leung, P.-H.; Hor, T. S. A. *J. Organomet. Chem.* **1994**, *476*, C32.

0020-1669/95/1334-6425$09.00/0 © 1995 American Chemical Society

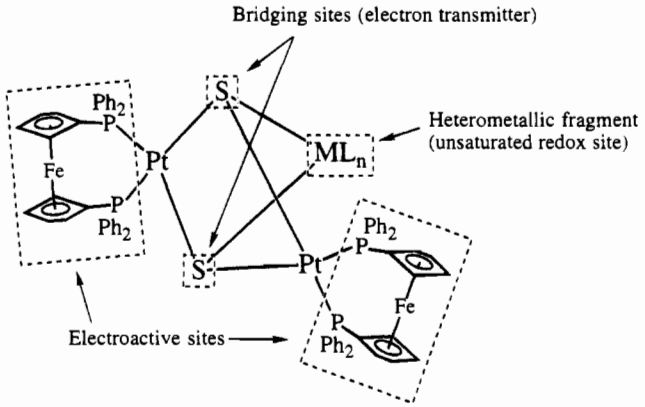

Figure 1. Structural representation of the intermetallic complex $Pt_2(dppf)_2(\mu_3\text{-}S)_2ML_n$ showing the different functional sites.

acid such as $TlNO_3$ in an approach to assemble an electroactive heteropolymetallic. The structure and electrochemistry of the resultant complex are described and compared with those of its PPh_3 derivative.[6] The synthetic method is general and can be extended to other main group Lewis acids.

Results and Discussion

Treatment of $TlNO_3$ with an equimolar amount of **2** gave a product formulated as $[Pt_2Tl(\mu_3\text{-}S)_2(dppf)_2]NO_3$ (**3a**), which

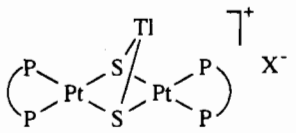

(P⌒P = dppf, X = NO_3, **3a**, PF_6, **3b**;

P⌒P = 2 x PPh_3, X = PF_6, **4**)

metathesizes with NH_4PF_6 to give $[Pt_2Tl(\mu_3\text{-}S)_2(dppf)_2]PF_6$ (**3b**). The IR spectrum of the latter gives the expected bands due to ionic PF_6^-. Conductivity measurements pointed to a 1:1 electrolyte in solution. The ^{31}P NMR spectrum gives δ_P and J_{Pt-P} values expected for a diplatinum moiety of $[Pt_2(dppf)_2(\mu\text{-}S)_2]$ and indicates that the two dppf ligands are chemically equivalent.

The solid-state structure of the PPh_3 analogue, **4**, has an intriguing "Mexican hat-like" structure.[6] In order to examine whether this unexpected structure can be maintained when the supporting ligands have changed, a single-crystal X-ray diffraction study was carried out on **3b** (Tables 1 and 2). The results indicated a remarkably similar configuration with a two-coordinated Tl^I suspended on the $\{Pt_2S_2\}$ core exposing a "vacant site" (Figure 2). The differences of dppf and PPh_3 in their coordination modes and electronic and steric demands do not impart any significant differences in the bonding parameters

Table 1. Crystallographic Data for $[Pt_2Tl(dppf)_2(\mu_3\text{-}S)_2]PF_6$

chemical formula	$[Pt_2Tl\{(C_5H_4PPh_2)_2Fe\}_2(S)_2]PF_6$
fw	1912.3
space group	*P2/n*
a, Å	17.795(4)
b, Å	10.553(2)
c, Å	17.936(4)
β, deg	107.09(3)
V, Å^3	3220(2)
Z	2
T, K	298
λ(Mo K), Å	0.710 73
ρ_{calc}, g/cm^3	1.973
μ, mm^{-1}	7.512
no. of obsd rflns	4308 ($\|F\| > 4.0\sigma(\|F\|)$)
$R(F_o)^a$	0.038
$R_w(F_o)^b$	0.044

^{a} $R = [\sum|F_o| - |F_c|]/\sum|F_o|$. ^{b} $R_w = [\sum w^2(|F_o| - |F_c|)^2/\sum w^2(|F_o|^2]^{1/2}$.

Table 2. Atomic Coordinates ($\times 10^4$) and Equivalent Isotropic Displacement Coefficients of Selected Non-Hydrogen Atoms (Å^2 $\times$ 10^3)^a

	x	*y*	*z*	*U*(eq)
Tl(1)	2500	−941(1)	2500	77(1)
Pt(1)	3281(1)	1871(1)	2194(1)	28(1)
Fe(1)	5267(1)	2095(1)	1331(1)	46(1)
S(1)	1956(1)	1228(2)	1644(1)	36(1)
P(1)	4521(1)	2565(2)	2827(1)	34(1)
P(2)	3284(1)	2378(2)	952(1)	31(1)
P(10)	2500	3829(7)	7500	96(2)
F(11)	3239(6)	3896(19)	8182(5)	245(10)
F(12)	2878(9)	2928(21)	7110(11)	308(13)
F(13)	2902(11)	4722(23)	7099(9)	311(13)
C(111)	5267(4)	1931(9)	2439(4)	42(3)
C(112)	6001(5)	2424(11)	2411(5)	54(4)
C(113)	6350(6)	1552(14)	2024(6)	75(5)
C(114)	5867(6)	478(12)	1824(6)	71(5)
C(115)	5185(6)	677(9)	2082(5)	52(4)
C(211)	4183(4)	2650(8)	681(4)	39(3)
C(212)	4693(5)	3716(9)	892(5)	50(3)
C(213)	5331(5)	3512(13)	574(6)	70(5)
C(214)	5213(6)	2365(12)	181(5)	65(4)
C(215)	4510(5)	1808(10)	245(5)	52(3)

^{a} Equivalent isotropic *U* defined as one-third of the trace of the orthogonalized U_{ij} tensor.

of the $\{Pt_2TlS_2\}$ chromophore (Tl−S 2.768(2) in **3b** vs 2.764(3) Å in **4**; ∠S−Tl−S 68.4(1)° vs 68.9(1)°; ∠Pt−Tl-Pt 57.8(1)° vs 58.3°) (Table 3). This affirms that the unique geometry adopted by the heterometal, *viz.* Tl, is largely a result of the juxtaposition of the two sulfide donors apart from the geometric preference of Tl^I. The negligible influence of the peripheral phosphines on the structural assembly allows us to tune the redox efficiency of these intermetallics without altering their molecular configurations.

One surprising feature of **3b** in its ^{195}Pt NMR spectrum is its doublet of triplets splitting (Figure 3). This is suggestive of a first-order pattern of an $A_2A_2'MM'X$ system with, apart from the usual P−Pt coupling, strong Pt−Tl spin−spin coupling (^2J(Pt−Tl) 1961 Hz).[7] This coupling is intriguing since no active metal−metal bonding is expected between the square-planar d^8 Pt^{II} and angular s^2 Tl^I in **3b**.[8] The Pt−Tl nonbonding but close contacts of 3.389(1) Å give strong support to this coupling. This distance is just outside the range expected for direct Pt−Tl bonds (e.g., 2.911(2) and 2.958(2) Å in $[Tl(crown\text{-}P_2)Pt(CN)_2]NO_3$, 3.085(1) Å in *cis*-$[(NH_3)_2Pt(1\text{-}MeT)_2Tl(1\text{-}$

(4) Gan, K.-S.; Hor, T. S. A. in *Ferrocenes—Homogeneous Catalysis, Organic Synthesis, Materials Science*; Togni, A., Hayashi, T., Eds.; VCH: Weinheim, Germany, 1995; p 3.

(5) Zanello, P. In *Ferrocenes—Homogeneous Catalysis, Organic Synthesis, Materials Science*; Togni, A., Hayashi, T., Eds.; VCH: Weinheim, Germany, 1995; p 317. Onaka, S.; Haga, M.-A.; Takagi, S.; Otsuka, M.; Mizuno, K. *Bull. Chem. Soc. Jpn.* **1994**, *67*, 2440. Watson, W. H.; Nagl, A.; Hwang, S.; Richmond, M. G. *J. Organomet. Chem.* **1993**, *445*, 163. Estevan, F.; Lahuerta, P.; Latorre, J.; Peris, E.; Garcia-Granda, S.; Gomez-Beltran, F.; Aguirre, A.; Salvado, M. A. *J. Chem. Soc., Dalton Trans.* **1993**, 1681. Pilloni, G.; Longato, B. *Inorg. Chim. Acta* **1993**, *208*, 17.

(6) Zhou, M.; Xu, Y.; Koh, L.-L.; Mok, K. F.; Leung, P.-H.; Hor, T. S. A. *Inorg. Chem.* **1993**, *32*, 1875.

(7) The observed coupling is between ^{195}Pt (N = 33.8%; I = $^1/_2$) and ^{203}Tl (N = 29.5%, I = $^1/_2$)/^{205}Tl (N = 70.5%, I = $^1/_2$). Couplings to the different Tl isotopes cannot be resolved.

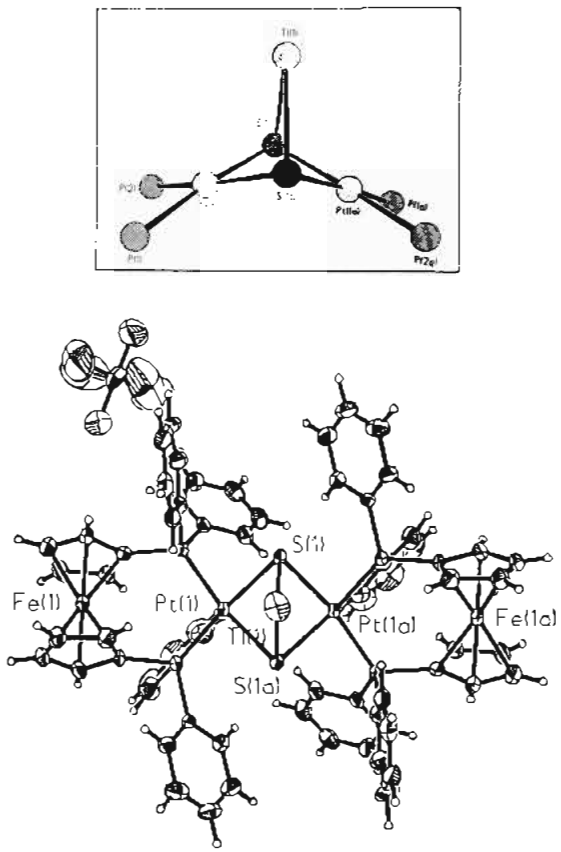

Figure 2. ORTEP structure of $[Pt_2Tl(dppf)_2(\mu_3\text{-}S)_2]PF_6$ (**3b**) with the inset showing the molecular drawing of the skeletal atoms.

Table 3. Selected Bond Distances (Å) and Angles (deg)

	Distances		
Tl(1)···Pt(1)	3.389(1)	Tl(1)−S(1)	2.768(2)
Tl(1)···Pt(1A)	3.389(1)	Tl(1)−S(1A)	2.768(2)
Pt(1)−S(1)	2.371(2)	Pt(1)−P(1)	2.286(2)
Pt(1)−P(2)	2.291(2)	Pt(1)−S(1A)	2.346(2)
Pt(1A)−S(1)	2.346(2)	Fe(1)−C(111−115)	2.036(9) (mean)
Fe(1)−C(211−215)	2.039(9) (mean)	P(10)−F(11−13A)	1.49(2) (mean)
	Angles		
S(1)−Tl(1)−S(1A)	68.4(1)	S(1)−Pt(1)−S(1A)	82.6(1)
Tl(1)−S(1)−Pt(1)	82.1(1)	Tl(1)−S(1)−Pt(1A)	82.6(1)
Pt(1)−S(1)−Pt(1A)	87.9(1)	P(1)−Pt(1)−S(1)	174.3(1)
P(2)−Pt(1)−S(1)	87.1(1)	P(2)−Pt(1)−S(1A)	169.6(1)
P(1)−Pt(1)−S(1A)	92.9(1)	P(1)−Pt(1)−P(2)	97.5(1)
Pt(1)···Tl(1)···Pt(1A)	57.8(1)		

$MeT)_2Pt(NH_3)_2]NO_3 \cdot 7H_2O$,[9] 3.034(1)−3.047(1) Å in $[TlPt_3(CO)_3(PCy_3)_3][Rh(\eta\text{-}C_8H_{12})Cl_2]$,[10] and 3.140(1) Å in $Tl_2Pt(CN)_4$).[11] The capping sulfide ligands are primarily responsible for juxtaposing the Tl^I atom in close vicinity of the Pt^{II} cores. They may also facilitate the through-bond spin−spin interaction between Pt and Tl as long-range coupling across the sulfur centers in these systems are well-known.[12] Nevertheless, the observed coupling is understandably weaker than that found in $[Tl(crown\text{-}P_2)Pt(CN)_2]NO_3$ (^1J(Pt−Tl) 3825 Hz)[13] in which direct Pt−Tl bond is proposed.

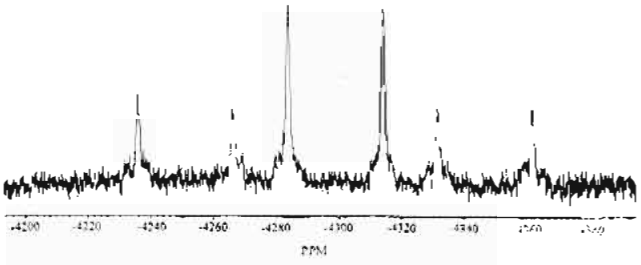

Figure 3. ^{195}Pt NMR spectrum of $[Pt_2Tl(dppf)_2(\mu_3\text{-}S)_2]PF_6$ (64.5 MHz) in CD_2Cl_2 showing the $J(^{31}P-^{195}Pt)$ and $^2J(^{195}Pt-^{203/205}Tl)$ couplings.

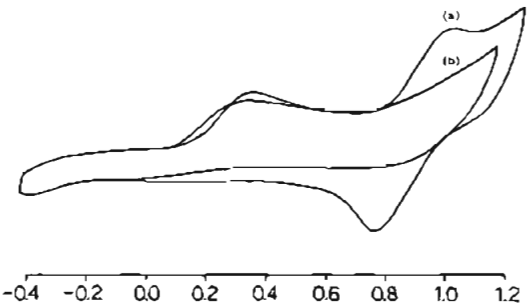

Figure 4. Cyclic voltammogram (0.2 V/s) for oxidation of 1.0 mM (a) $[Pt_2Tl(dppf)_2(\mu_3\text{-}S)_2]PF_6$ and (b) $[Pt_2Tl(PPh_3)_4(\mu_3\text{-}S)_2]PF_6$ in 1,2-dichloroethane at Pt electrode with $Bu_4N^+ClO_4^-$ (0.2 M) as supporting electrolyte.

The chelate angle P−Pt−P (97.5(1)°) is the smallest among the Pt^{II} complexes with chelating dppf.[4] This angle reportedly spans a wide range from 93.6° in *fac*-$ReCl(CO)_3(dppf)$[14] and $[Ir(dppf)_2]BPh_4$[15] to as high as 117.8° in $Cu_2(\mu\text{-}NO_3)_2(dppf)_2$.[16] Such an adjustable bite allows the diphosphine to stabilize metal fragments of different geometries and levels of coordination saturation. This inherent flexibility may be the prime reason why many dppf complexes are catalytically active.[4] In **3b**, the small bite is accompanied by an ideal staggered (*gauche*) conformation (36°) with the two C_5 rings subtending a small angle of 4.9° to each other.

The cyclovoltammetry behavior of **3b**, examined in 1,2-dichloroethane, shows an irreversible anodic peak at +0.32 V and a pair of redox wave at $E_{1/2}$ = 0.89 V (Figure 4a). The former corresponds to the oxidation of the Tl^I center. This compares well with the voltammogram (E_{pa} = +0.29 V) obtained for **4** (Figure 4b). Since only one redox wave was observed for the ferrocenyl moieties, the possibility of a simultaneous two-electron oxidation, one from each Fe^{II} center, was examined. Such a process would be expected to yield a 30 mV peak-to-peak separation. However, 180 mV is observed

(8) It has been reported that direct metal−metal bonds between $6s^2$ metals such as Pb^{II} and Tl^I and d^8 Pt^{II} as in $[(OAc)Pb(crown\text{-}P_2)Pt(CN)_2]OAc$ and $Tl_2Pt(CN)_2$ can occur. However, this is based on a columnar or pseudooctahedral model with σ overlap between the filled $5d_{z^2}$ and the empty $6p_z$ valence orbitals on Pt^{II} and the filled 6s and empty $6p_z$ valence orbitals of the main group metal. (Refer to ref 11b and: Balch, A. L.; Fung, E. Y.; Nagle, J. K.; Olmstead, M. M.; Rowley, S. P. *Inorg. Chem.* **1993**, *32*, 3295.) The Tl^I center in **3** is significantly off the axial plane of the Pt^{II} local sphere but on the C_2 axis of the diplatinum moiety.

(9) Renn, O.; Lippert, B.; Mutikainen, I. *Inorg. Chim. Acta* **1993**, *208*, 219.

(10) Ezomo, O. J.; Mingos, D. M. P.; Williams, I. D. *J. Chem. Soc., Chem. Commun.* **1987**, 924.

(11) (a) Nagle, J. K.; Balch, A. L.; Olmstead, M. M. *J. Am. Chem. Soc.* **1988**, *110*, 319. (b) Ziegler, T.; Nagle, J. K.; Snijders, J. G.; Baerends, E. J. *J. Am. Chem. Soc.* **1989**, *111*, 5631.

(12) Hor, T. S. A. *D. Phil. Thesis*, University of Oxford, Oxford U.K., 1983. Briant, C. E.; Gardner, C. J.; Hor, T. S. A.; Howells, N. D.; Mingos, D. M. P. *J. Chem. Soc., Dalton Trans.* **1984**, 2645. Gukathasan, R. R.; Morris, R. H.; Walker, A. *Can. J. Chem.* **1983**, *61*, 2490.

(13) Balch, A. L.; Rowley, S. P. *J. Am. Chem. Soc.* **1990**, *112*, 6139.

(14) Miller, T. M.; Ahmed, K. J.; Wrighton, M. S. *Inorg. Chem.* **1989**, *28*, 2347.

(15) Casellato, U.; Corain, B.; Graziani, R.; Longato, B.; Pilloni, G. *Inorg. Chem.* **1990**, *29*, 1193.

(16) Neo, S. P.; Zhou, Z.-Y.; Mak, T. C. W.; Hor, T. S. A. *J. Chem. Soc., Dalton Trans.* **1994**, 3451.

for **3b** compared to 120 mV for the $[FeCp_2]^+/FeCp_2$ couple and 100 mV for the $[PtCl_2(dppf)]^+/PtCl_2(dppf)$ couple. This suggests that the redox process in **3b** is quasi-reversible under the experimental conditions. Besides, the observation of a single cyclic voltammetric wave for the oxidation of both ferrocenyl centers suggests that the two sites are not in charge-transfer communication. In order to confirm this, two related complexes with $[InCl_3]$ and $[Pb(NO_3)]$ as the heterometallic fragments, *viz.* $Pt_2(dppf)_2(\mu_3\text{-}S)_2InCl_3$, (**5**) and $[Pt_2(dppf)_2(\mu_3\text{-}S)_2Pb(NO_3)]NO_3$

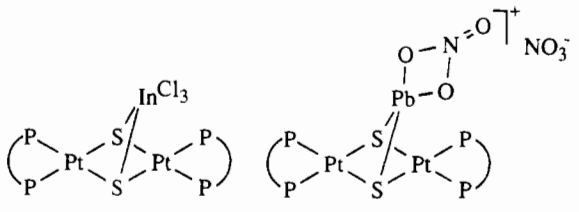

(P⌒P = dppf, **5**) (P⌒P = dppf, **6**)

(**6**), were synthesized and their cyclovoltammetry was studied. Spectroscopic and conductivity data suggested that both complexes are isostructural to their PPh_3 counterparts, which were reported recently.[2] Complex **5** is covalent but dissociates readily in solution to give a 1:1 electrolyte. The redox potentials of the coordinated dppf ligands in **5** ($E_{pa} = 0.99$, $E_{pc} = 0.82$ V) and **6** ($E_{pa} = 1.01$, $E_{pc} = 0.84$ V) are very similar to that in **3b** ($E_{pa} = 0.97$, $E_{pc} = 0.79$ V). The charge-transfer communication between the two dppf sites in these intermetallics is therefore minimum.

The similar peak area of the first anodic peak and the cathodic peak of two dppf ligands indicated that the Tl^I center is oxidized to Tl^{III} through a two-electron-transfer process. This is interpreted as the sequential oxidation from the initial state of $[(dppf)\cdots Tl^+\cdots(dppf)]$ to $[(dppf)\cdots Tl^{3+}\cdots(dppf)]$ followed by $[(dppf)^+\cdots Tl^{3+}\cdots(dppf)^+]$. During the reverse cathodic scan, the intermediate species $[(dppf)\cdots Tl^{3+}\cdots(dppf)]$ is regenerated. However, it cannot be reversibly reduced, as indicated by the absence of the coupled cathodic peak and the defeaturing of the voltammogram where the peaks are flattened after several scans. This is attributed to the irreversible adsorption of the product on the electrode surface giving a layer of inert film which hinders further electrochemical reactions. The dull-colored poisoned Pt electrode can be revived upon polishing and the voltammetric profile of **3b** restored.

Conclusion

Heterometallic complexes with the ability to display sequential multistepped electron transfers are known to show some unusual catalytic properties.[17] It is also worth pointing out that dppf is among the best diphosphine ligands to promote the catalytic activity of metal complexes.[4] Isolation of these intermetallic complexes therefore provides a platform for these two ideas to be integrated. The demonstration of these ideas is a subject of our future reports.

Experimental Section

All preparations were routinely carried out under dry argon atmosphere and in dry oxygen-free solvents. $Pt_2(dppf)_2(\mu\text{-}S)_2$ was synthesized from $PtCl_2(dppf)$ or $[Pt(dppf)(CH_3CN)_2][BF_4]_2$.[3] Elemental analyses were performed by the Microanalytical Laboratory in our Department. The presence of CH_2Cl_2 solvate was confirmed by ^1H NMR analysis.

Infrared spectra were obtained as a KBr disk by using a Shimadzu IR-470 spectrometer. Routine ^1H, ^{31}P and ^{195}Pt NMR spectra were recorded in $CDCl_3$ solutions at 25 °C on a Bruker ACF 300 spectrometer. Conductivities were measured using a Horiba ES-12 conductivity meter. Voltammetric measurements were carried out by a Hokuko Dento HA-303 potentiostat with a Hokuko Dento HB 104 function generator and a Graphtec WX 2400 XY recorder. All electrochemical experiments were performed in dry and freshly distilled 1,2-dichloroethane with 0.2 M tetrabutylammonium perchlorate as supporting electrolyte using a three-electrode cell. A silver/silver nitrate (0.1 M) electrode in acetonitrile was used as reference electrode while Pt wires were used as working and counter electrodes.

Preparation of $[Pt_2Tl(\mu_3\text{-}S)_2(dppf)_2]X$ (X = NO_3, 3a, and PF_6, 3b). $TlNO_3$ (0.037 g, 0.139 mmol) was added to a suspension of $Pt_2(dppf)_2(\mu\text{-}S)_2$ (0.217 g, 0.139 mmol) in MeOH (50 mL) and the mixture stirred for 1 h. The resultant orange solution was filtered, concentrated to low volume, and cooled to precipitate orange microcrystals of $[Pt_2Tl(\mu_3\text{-}S)_2(dppf)_2]NO_3$ (0.224 g, 88%). Anal. Calcd: C, 44.64; H, 3.06; Fe, 6.13; N, 0.76; P, 6.78; Pt, 21.33; S, 3.50. Found: C, 44.93; H, 3.33; Fe, 5.76; N, 0.61; P, 6.66; Pt, 21.00; S, 3.39. ^{31}P NMR (ppm): δ 18.34 (J(P−Pt) 3042, ^3J(P−Pt) 25 Hz) ($CDCl_3$); 18.16 (J(P−Pt) 3060, ^3J(P−Pt) 24 Hz) (CD_2Cl_2). Λ_m (10^{-3} M): 85.5 Ω^{-1} cm^2 mol^{-1} (CH_3OH). The PF_6^- salt was prepared by adding slowly with stirring a MeOH solution of NH_4PF_6 in excess to a concentrated solution of the nitrate complex in MeOH. The resultant precipitate was isolated by filtration, washed with MeOH, and recrystallized from CH_2Cl_2/hexane. Anal. Calcd: C, 42.69; H, 2.93; F, 5.96; Fe, 5.84; P, 8.11; Pt, 20.41; S, 3.36. Found: C, 43.41; H, 2.84; F, 6.25 Fe, 5.02; P, 8.11; Pt, 19.65; S, 3.31. ^{31}P NMR (ppm): δ 18.03 (J(P−Pt) 3083, ^3J(P−Pt) 23 Hz) ($CDCl_3$); 18.01 (J(P−Pt) 3091, ^3J(P−Pt) 23 Hz) (CD_2Cl_2). ^{195}Pt NMR (ppm): δ −4299 (J(P−Pt) 3092, J(Pt−Tl) 1961 Hz). IR: $\nu(PF_6^-)$ 838 cm^{-1}. Λ_m (10^{-3} M): 64.4 (CH_2Cl_2); 80.4 Ω^{-1} cm^2 mol^{-1} (CH_3OH).

Preparation of $Pt_2(dppf)_2(\mu_3\text{-}S)_2InCl_3$ (5). $InCl_3$ (0.022 g, 0.098 mmol) was added to a suspension of $Pt_2(dppf)_2(\mu\text{-}S)_2$ (0.154 g, 0.098 mmol) in MeOH (50 mL) and the mixture stirred for 4 h. The resultant orange yellow solution was filtered and evaporated to dryness. The residue was redissolved in CH_2Cl_2, filtered, and concentrated and hexane added to give an orange crystalline product analyzed as $Pt_2(dppf)_2(\mu_3\text{-}S)_2InCl_3\cdot{}^1/_3CH_2Cl_2$ (0.106 g, 61%). Anal. Calcd: C, 45.33; H, 3.15; Cl, 7.05; Fe, 6.17; In, 6.34; P, 6.85; Pt, 21.56; S, 3.54. Found: C, 45.22; H, 3.15; Cl, 7.65; Fe, 6.17; In, 6.19; P, 6.84; Pt, 21.41; S, 3.85. ^{31}P NMR (ppm): δ 17.74 (J(P−Pt) 3170, ^3J(P−Pt) 18 Hz) ($CDCl_3$). In CD_3OD, it dissolves and dissociates to give $[Pt_2(dppf)_2(\mu_3\text{-}S)_2InCl_2]Cl$. ^{31}P NMR: δ 18.28 (J(P−Pt) 3226) (CD_3OD). Λ_m (10^{-3} M): 1.6 (CH_2Cl_2); 72.2 Ω^{-1} cm^2 mol^{-1} (CH_3OH).

Preparation of $[Pt_2(dppf)_2(\mu_3\text{-}S)_2Pb(NO_3)]NO_3$ (6). A procedure similar to that for **5** was used with $Pb(NO_3)_2$ (0.051 g, 0.189 mmol) and $Pt_2(dppf)_2(\mu\text{-}S)_2$ (0.296 g, 0.189 mmol). The product was analyzed as $[Pt_2(dppf)_2(\mu_3\text{-}S)_2Pb(NO_3)]NO_3\cdot CH_2Cl_2$ (0.231 g, 67%). Anal. Calcd: C, 41.27; H, 2.85; Fe, 5.64; N, 1.42; P, 6.26; Pb, 10.47; Pt, 19.71; S, 3.24. Found: C, 41.02; H, 2.95; Fe, 5.31; N, 2.43; P, 6.60; Pb, 8.96; Pt, 17.53; S, 3.35. ^{31}P NMR (ppm): δ 15.76 (J(P−Pt) 3198). Λ_m (10^{-3} M): 9.5 (CH_2Cl_2); 81.8 Ω^{-1} cm^2 mol^{-1} (CH_3OH).

Crystal Structure Determination and Refinement. Orange crystals of $[Pt_2Tl(\mu_3\text{-}S)_2(dppf)_2]PF_6$ suitable for single-crystal X-ray structural determination were grown by slow diffusion of hexane into a solution of **3b** in CH_2Cl_2. A single crystal of 0.40 × 0.30 × 0.10 mm was chosen for the X-ray diffraction study with Mo Kα (λ 0.710 73 Å) radiation at room temperature. The crystal data and experimental conditions are given in Table 1. Atomic coordinates and equivalent isotropic displacement coefficients are given in Table 2. A total of 5633 ($3.5° < 2\theta < 50.0°$) independent reflections were measured by scanning on a Siemens R3m/V four-circle diffractometer with a beam monochromator. The intensity data were reduced and corrected for Lorentz and polarization factors using the applied programs. The absorption correction was made with ψ scans on reflections (1 2 1), (0 −3 0), (0 4 1), (2 4 1) and (2 4 3). The function minimized was $\sum w(F_o - F_c)^2$. The unit cell constants were determined by the least-square

(17) Hayashi, T. In *Ferrocenes—Homogeneous Catalysis, Organic Synthesis, Materials Science*; Togni, A., Hayashi, T., Eds.; VCH: Weinheim, Germany, 1995; p 105. Butsugan, Y.; Araki, S.; Watanabe, M. *Ibid.* p 143. Kumada, M. *Pure Appl. Chem.* **1980**, *52*, 669. Hayashi, T.; Konishi, M.; Yokota, K.-I.; Kumada, M. *J. Chem. Soc., Chem. Commun.* **1981**, 313. Hayashi, T.; Kumada, M. *Acc. Chem. Res.* **1982**, *15*, 395. Hughes, O. H.; Unruh, J. D. *J. Mol. Catal.* **1981**, *12*, 71. Fellman, J. D.; Garrou, P. E.; Wither, H. P.; Seyferth, D.; Traficante, D. D. *Organometallics* **1983**, *2*, 818.

fits to the setting parameters of 20 independent reflections in the range of $4.78° < 2\theta < 21.21°$.

The crystal structure was solved with the XS program of SHELXTL-PLUS[18] by using a DEC MicroVax-II minicomputer and refined by full-matrix least-squares analysis with the SHELXTL-PC programs on an IBM-compatible 486 PC. The positions of the heavier atoms Tl, Pt, Fe, and S were first located by direct methods. P, F, and C atoms were located from difference maps. Non-hydrogen atoms were refined anisotropically. All hydrogen atoms were placed at calculated positions with fixed isotropic thermal parameters. Final refinement gave $R = 0.038$, $wR = 0.044$, goodness of fit = 1.26, $\Delta\rho_{min} = -1.42$ eÅ^{-3}. The atomic coordinates of non-hydrogen atoms are given in Table 2.

(18) Siemens Analytical X-Ray Instruments, Inc., Madison, WI, 1989.

Acknowledgment. This work was generously supported by the National University of Singapore (Grant RP 850030). We thank M. O. Wong for experimental assistance, the technical staff of the department for professional support, and Y. P. Leong for stenographic work.

Supporting Information Available: Tables giving details of the X-ray structure analysis, crystallographic data, refined atomic coordinates and isotropic thermal parameters, bond lengths, bond angles, anisotropic displacement coefficients, and hydrogen atom coordinates, and isotropic displacement coefficients and crystal structure (10 pages). Ordering information is given on any current masthead page.

IC950690L